# A new take on FWI: Wavefield Reconstruction Inversion

T. van Leeuwen[1], F.J. Herrmann[2] and B. Peters[2]
[1]Centrum Wiskunde & Informatica, Amsterdam, The Netherlands
[2]University of British Columbia, dept. of Earth, Ocean and Atmospheric Sciences, Vancouver, Canada.

January 14, 2014

**Abstract**

We discuss a recently proposed novel method for waveform inversion: Wavefield Reconstruction Inversion (WRI). As opposed to conventional FWI – which attempts to minimize the error between observed and predicted data obtained by solving a wave equation – WRI reconstructs a wave-field from the data and extracts a model-update from this wavefield by minimizing the wave-equation residual. The method does not require explicit computation of an adjoint wavefield as all the necessary information is contained in the reconstructed wavefield. We show how the corresponding model updates can be interpreted physically analogously to the conventional imaging-condition-based approach.

## Introduction

Recently, van Leeuwen and Herrmann (2013) introduced a novel approach to full-waveform inversion (FWI). Where the conventional approach to FWI is typically based on an output-error formulation such as output least-squares (OLS) (Tarantola, 1984; Pratt et al., 1998), the approach proposed by van Leeuwen and Herrmann (2013) is more closely related on an equation-error (EE) approach. The main difference between these two approaches can be illustrated as follows. We are interested in identifying the parameters $\mathbf{m}$, given the output $\mathbf{d}$ of a system $F$, i.e., $\mathbf{d} = F(\mathbf{m})$. In this case we consider $F(\mathbf{m}) = P\mathbf{u}$ where $A(\mathbf{m})\mathbf{u} = \mathbf{q}$ encodes the underlying physics through a (discretized) PDE $A$ with coefficients $\mathbf{m}$ and source term $\mathbf{q}$. $P$ is the observation operator which samples the solution of the PDE at the receiver locations. The OLS approach aims to find the parameters for which the predicted output $P\mathbf{u}$ – obtained by solving the PDE (i.e., $\mathbf{u} = A^{-1}(\mathbf{m})\mathbf{q}$) – matches the measurements:

$$\min_{\mathbf{m}} ||PA^{-1}(\mathbf{m})\mathbf{q} - \mathbf{d}||_2^2. \tag{OLS}$$

The EE approach, on the other hand, aims to minimize the error in the constitutive equation given an estimate of the field obtained from the data (i.e., $\mathbf{u} = P^{-1}\mathbf{d}$):

$$\min_{\mathbf{m}} ||A(\mathbf{m})P^{-1}\mathbf{d} - \mathbf{q}||_2^2. \tag{EE}$$

The fundamental difference between the two approaches is the way the objective depends on $\mathbf{m}$; through $A^{-1}$ or through $A$. The EE approach is often used for identifying diffusion coefficients (Hanke and Scherzer, 1998) or in stready-state elastodynamics (Banerjee et al., 2013), where a *complete* measurement of the state variable $\mathbf{u}$ is available (i.e., $P$ is invertible). Of course, in seismic imaging we typically have *incomplete* measurements of the wavefield and the EE approach is not directly applicable.

The method proposed by van Leeuwen and Herrmann (2013) is a way of bootstrapping the EE approach by estimating the wavefield and model parameters in an alternating fashion. The wavefield is estimated by demanding that it solves the wave-equation for the current model *and* fits the data. This leads to an overdetermined system of equations which we dub the *data-augmented wave-equation*, which is solved in a least-squares sense. This wavefield is then used as input for the EE approach, yielding a new estimate for the model parameters. Since this method hinges on reconstructing the wavefield and subsequently extracting information from it, we will refer to it as Wavefield Reconstruction Inversion (WRI). Preliminary results suggest that this approach may alleviate some of the problems with local minima in FWI because it effectively enlarges the search-space. Moreover, the method does not require explicit computations of an adjoint wavefield.

In this paper, we briefly review the method introduced by van Leeuwen and Herrmann (2013) and present some illustrative examples in order to provide some intuition into the underlying mechanisms. We draw parallels between the conventional adjoint-state approach and high-light the main differences. Further numerical examples are presented in a companion abstract.

## Theory

The alternating approach outlined above can be mathematically formalized by considering the following optimization problem where the wave equation is added as a penalty term to the data-misfit

$$\min_{\mathbf{m},\mathbf{u}} ||P\mathbf{u} - \mathbf{d}||_2^2 + \lambda^2||A(\mathbf{m})\mathbf{u} - \mathbf{q}||_2^2. \tag{1}$$

Since optimization over the full space $(\mathbf{m}, \mathbf{u})$ is not computationally feasible, we eliminate the wavefield by minimizing the above objective w.r.t. $\mathbf{u}$ for a fixed $\mathbf{m}$. This can be done by solving

$$\left(\lambda^2 A(\mathbf{m})^* A(\mathbf{m}) + P^*P\right)\mathbf{u} = \lambda^2 A(\mathbf{m})^*\mathbf{q} + P^*\mathbf{d}. \tag{2}$$

In this *data augmented wave-equation* we recognize the original wave equation, as well as additional contributions given by the data. We denote the solution by $\bar{\mathbf{u}}_\lambda$ and define the following reduced objective

$$\phi_\lambda(\mathbf{m}) = ||P\bar{\mathbf{u}}_\lambda - \mathbf{d}||_2^2 + \lambda^2 ||A(\mathbf{m})\bar{\mathbf{u}}_\lambda - \mathbf{q}||_2^2. \tag{3}$$

The corresponding gradient is given by

$$\nabla\phi_\lambda(\mathbf{m}) = G(\mathbf{m},\bar{\mathbf{u}}_\lambda)^*\bar{\mathbf{v}}_\lambda, \tag{4}$$

where $G(\mathbf{m},\mathbf{u})$ is the Jacobian of $A(\mathbf{m})\mathbf{u}$ and $\bar{\mathbf{v}}_\lambda = \lambda^2(A(\mathbf{m})\bar{\mathbf{u}}_\lambda - \mathbf{q})$.

The conventional least-squares objective and its gradient are given by

$$\begin{aligned} \phi(\mathbf{m}) &= ||P\bar{\mathbf{u}} - \mathbf{d}||_2^2, & (5)\\ \nabla\phi(\mathbf{m}) &= G(\mathbf{m},\bar{\mathbf{u}})^*\bar{\mathbf{v}}, & (6) \end{aligned}$$

where $A(\mathbf{m})\bar{\mathbf{u}} = \mathbf{q}$ and $A(\mathbf{m})^*\bar{\mathbf{v}} = P^*(P\bar{\mathbf{u}} - \mathbf{d})$.

The gradient of both objectives have the same structure (cf. eqs. 4 and 6 ); it is a 'correlation' of a forward wavefield and an adjoint wavefield. But whereas these wavefields have a well-defined physical meaning in the conventional method, it is not clear what the physical interpretation is of the wavefields $\bar{\mathbf{u}}_\lambda$ and $\bar{\mathbf{v}}_\lambda$. To shed some light on this matter we will first explore some relations between these wavefields and present some numerical examples in the next section. First, we state without proof that

$$\begin{aligned} \bar{\mathbf{u}}_\lambda &\approx \bar{\mathbf{u}} + \lambda^{-2}A(\mathbf{m})^{-1}\bar{\mathbf{v}}, & (7)\\ \bar{\mathbf{v}}_\lambda &\approx \bar{\mathbf{v}}, & (8)\\ \nabla\phi_\lambda &\approx \nabla\phi + \lambda^{-2}G(\mathbf{m},A(\mathbf{m})^{-1}\bar{\mathbf{v}})^*\bar{\mathbf{v}}. & (9) \end{aligned}$$

This indicates that as $\lambda \uparrow \infty$ we retrieve the conventional approach. For small values of $\lambda$, however, both the source wavefield and the gradient contain significant additional contributions from $A(\mathbf{m})^{-1}\bar{\mathbf{v}}$. In fact, is seems that the *data-augmented* wavefield now contains all the information necessary (i.e., both the incident field and the reflections) to form an image. To compute the image, this wavefield is correlated with $\bar{\mathbf{v}}_\lambda = A\bar{\mathbf{u}}_\lambda - \mathbf{q}$, which can be written as $\bar{\mathbf{v}}_\lambda = A(\bar{\mathbf{u}}_\lambda - \bar{\mathbf{u}})$. Thus, the incident wave is subtracted from $\bar{\mathbf{u}}_\lambda$ to form a wavefield containing only the reflections. The additional cross-term obtained from correlating the reflections with themselves is apparent in eq. (9).

**Illustrative examples**

*Imaging*

Just as the gradient of the least-squares objective in FWI yields an image, so does the gradient of the new objective (eq. 3). However, for the latter we do not need to compute an adjoint wavefield! All we need to compute the gradient is the *data-augmented* wavefield (eq. 2). To gain some insight in how this gradient builds up an image, we consider a simple two-layer model and plot snapshots (in time) of the wavefields, see figure 1. We observe that the *data-augmented* wavefield $\bar{\mathbf{u}}_\lambda$ indeed contains both the incident wave as well as the reflection!

*Inversion*

To illustrate the properties of the gradient-updates for inversion, we consider the model depicted in figure 2 (a). The corresponding wavefield is depicted in figure 2 (b). The wavefields $\bar{\mathbf{u}}_\lambda$ for a for a single frequency for various values of $\lambda$ as well the conventional wavefield are shown in figure 3 (top row). The corresponding predicted data as well as the observed data are shown in figure 3 (middle row). Note that by incorporating the observed data as constraint in the wave-equation, the cycle-skips have disappeared for $\lambda = 1$. Instead, the residual is smeared out over the entire domain as can be seen in the corresponding wavefield.

## Discussion & Conclusion

We have briefly reviewed a recently proposed novel method for waveform inversion: Wavefield Reconstruction Inversion (WRI). As opposed to conventional FWI – which attempts to minimize the error between observed and predicted data obtained by solving a wave equation – WRI reconstructs a wavefield from the data and extracts a model-update from this wavefield. The misfit for this new method consists of two terms; a data-misfit terms and a term that measures if the reconstructed wavefield obeys a wave-equation. As such, WRI can be seen as an extension of conventional FWI in the sense that it allows for wavefields that are *not* physically meaningful (Symes, 2013). Preliminary experiments (van Leeuwen and Herrmann, 2013) suggest that this method mitigates some of the problems with local minima in FWI.

As the reconstructed wavefield contains all the information necessary for constructing an update, no adjoint wavefield needs to be computed. However, this comes at the cost of having to solve an 'overdetermined' wave-equation, where the data act as additional constraints. In the frequency-domain, this can be done in a straightforward manner by solving a large sparse overdetermined system, for example with QR factorization. In the time-domain, the additional constraints turn the usual system of coupled ODEs into a differential algebraic equation (DAE) and special numerical solution techniques need to be applied to solve such equations (Petzold and Ascher, 1998).

We expect that WRI will be especially beneficial for multi-parameter inversion, since it separates the problem naturally in two parts; reconstructing the wavefield from the data, and extracting model parameters from the wavefield. The latter is exactly the regime for which the equation-error approach was developed, and existing methods may be adapted to perform such an inversion.

## Acknowledgments

This work was in part financially supported by the Natural Sciences and Engineering Research Council of Canada Discovery Grant (22R81254) and the Collaborative Research and Development Grant DNOISE II (375142-08). This research was carried out as part of the SINBAD II project with support from the following organizations: BG Group, BGP, BP, CGG, Chevron, ConocoPhillips, ION, Petrobras, PGS, Statoil, Total SA, WesternGeco, and Woodside.

## References

Banerjee, B., Walsh, T.F., Aquino, W. and Bonnet, M. [2013] Large Scale Parameter Estimation Problems in Frequency-Domain Elastodynamics Using an Error in Constitutive Equation Functional. *Computer methods in applied mechanics and engineering*, **253**, 60–72, ISSN 0045-7825, doi:10.1016/j.cma.2012.08.023.

Hanke, M. and Scherzer, O. [1998] Error Analysis of an Equation Error Method for the Identification of the Diffusion Coefficient in a Quasi-linear Parabolic Differential Equation. *SIAM Journal on Applied Mathematics*, **59**(3), 1012–1027, ISSN 0036-1399, doi:10.1137/S0036139997331628.

Petzold, L.R. and Ascher, U.M. [1998] *Computer methods for ordinary differential equations and differential-algebraic equations*, vol. 61. Siam.

Pratt, G., Shin, C. and Hicks, G. [1998] Gauss-Newton and full Newton methods in frequency-space seismic waveform inversion. *Geophysical Journal International*, **133**(2), 341–362, ISSN 0956540X, doi:10.1046/j.1365-246X.1998.00498.x.

Symes, W. [2013] Personal communication.

Tarantola, A. [1984] inversion of seismic reflection data in the acoustic approximation. *Geophysics*, **49**(8), 1259–1266.

van Leeuwen, T. and Herrmann, F.J. [2013] Mitigating local minima in full-waveform inversion by expanding the search space. *Geophysical Journal International*, doi:10.1093/gji/ggt258.

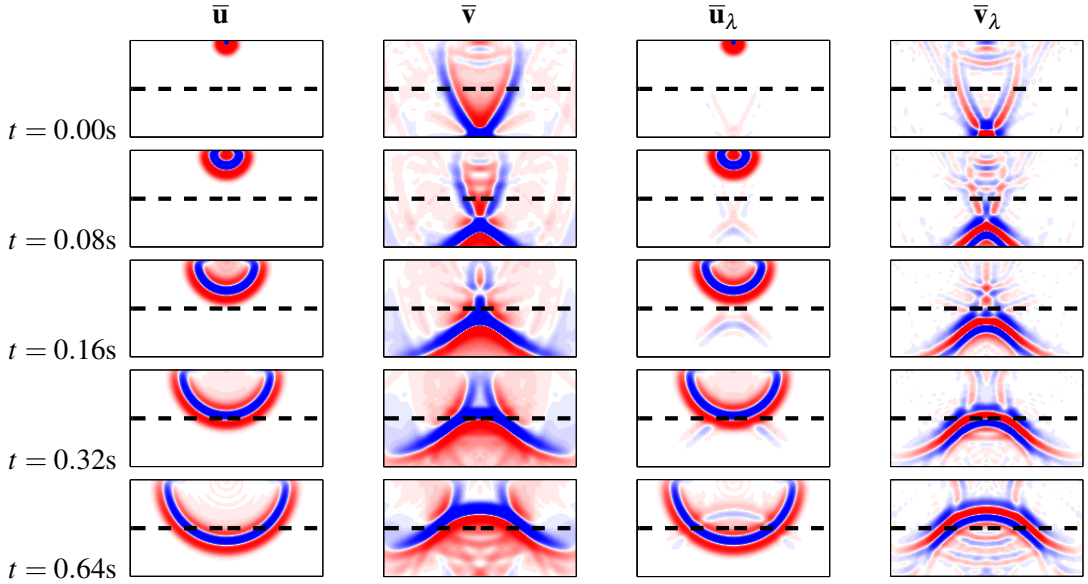


***Figure 1*** *Snapshots of wavefields for constant background velocity. The data where generated for a two-layer model (indicated with dashed line). The conventional forward and adjoint wavefields are shown in the left two panels. The wavefield obtained by solving the data-augmented wave-equation is shown in the third panel. There clearly is a reflected event present in the wavefield even though the background model was constant! The corresponding 'adjoint' wavefield is shown in the fourth panel and resembles the conventional adjoint wavefield.*

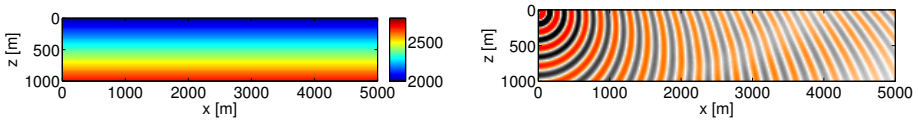


***Figure 2*** *(a) Velocity model and (b) corresponding wavefield at 10 Hz.*

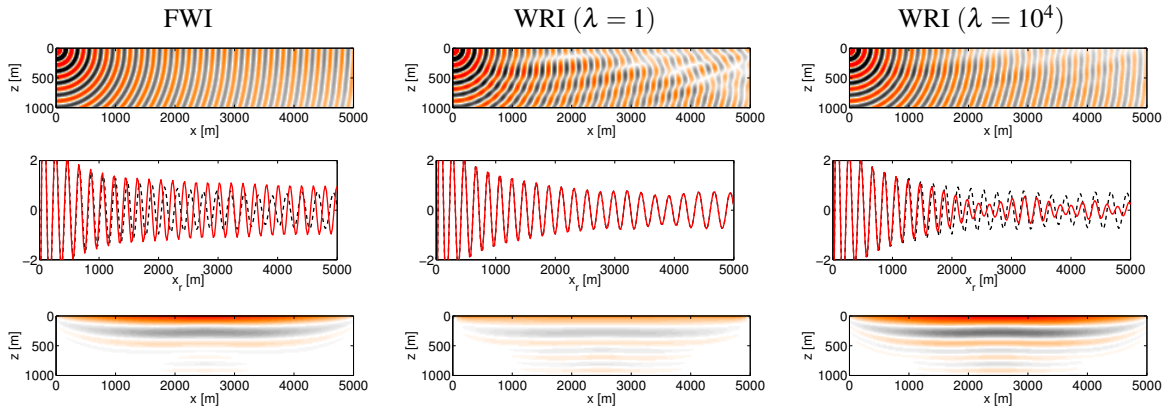


***Figure 3*** *The top row show the wavefields for a constant background velocity for FWI (left) and WRI for various values of $\lambda$. The middle row shows the corresponding data as well the observed data. Note that for $\lambda = 1$ the cycle-skips have dissappeared. Finally, the bottom row shows the resulting gradient updates.*